binding sites on carbohydrate chains. Carbohydrate moieties may participate in IL-1 binding to mammalian cell surface receptors (*13*). Soluble IL-1 receptors expressed in mammalian cells, but not bacteria or yeast, yield a product with the same binding affinity as that of the naturally occurring membrane receptor (*14*).

The nature of the IL-1 binding structure to *E. coli* is unclear, but the ability of the IL-1ra to block both the binding and the growth-promoting effect of IL-1 suggests that the bacterial binding structure recognizes both IL-1ra and IL-1. The binding of IL-1 to virulent strains of *E. coli* is specific and saturable and avirulent strains do not bind IL-1 under the same conditions. These binding data are consistent with the observation that IL-1 enhances the growth of virulent rather than avirulent strains of *E. coli*.

It is unlikely that the growth enhancement is a result of nutritional factors, because we observed enhanced growth in a highly enriched medium (BHI broth) as well as in a nutritionally limited medium (RPMI). Enrichment of the RPMI media with increasing concentrations of glucose did not affect IL-1–induced growth (*10*).

Although our data suggest that some bacteria can use IL-1 to increase their growth, the bacteria may also be a source of IL-1 or IL-1–like molecules. Some Gram-negative bacteria produce a protein that has IL-1–like activities, such as induction of serum amyloid A, granulocytic colony-stimulating activity, and the synthesis of IL-2 (*15*).

The significance of our findings for the progression of bacterial infections is unclear. Our data suggest that IL-1, produced in vivo as a result of inflammation or in the course of bacterial infection, could serve as a growth factor for virulent bacteria, thereby potentially worsening infection or the risk of infection. IL-1 does not alter the numbers of bacteria at the stationary phase, but rather affects the rate at which the stationary phase is reached. Certain antibacterial agents, for example, cell wall–active drugs, are more effective when bacteria are multiplying rapidly than when multiplying slowly. The importance for the outcome of infection or a more rapid attainment of the stationary phase by IL-1 is not known.


REFERENCES AND NOTES

1. C. A. Dinarello, *Blood* 77, 1627 (1991).
2. J. E. Sims *et al.*, *Science* **241**, 585 (1988).
3. S. Okusawa, J. A. Gelfand, T. Ikejima, R. J. Connolly, C. A. Dinarello, *J. Clin. Invest.* **81**, 1162 (1988).
4. G. Wakabayashi, J. A. Gelfand, J. F. Burke, R. C. Thompson, C. A. Dinarello, *FASEB J.* **5**, 338 (1991); K. Ohlsson, P. Bjork, M. Bergenfeldt, R. Hageman, R. C. Thompson, *Nature* **348**, 550 (1990).
5. W. R. McCabe, B. Kaijser, S. Olling, M. Uwaydeh, L. A. Hanson, *J. Infect. Dis.* **138**, 33 (1978).
6. R. J. Roantree and L. A. Rantz, *J. Clin. Invest.* **39**, 72 (1960).
7. *Escherichia coli* from blood, feces, or urine samples were obtained from the clinical microbiology laboratory, New England Medical Center.
8. R. Porat, M. A. Johns, W. R. McCabe, *Infect. Immun.* **55**, 320 (1987).
9. Human recombinant TNFα was from Genentech, Inc. (South San Francisco, CA), human recombinant IL-4 was from Schering, Inc. (Bloomington, NJ), human recombinant IL-1ra was from Synergen, Inc. (Boulder, CO), IL-1 receptor antagonist protein was from Upjohn Co. (Kalamazoo, MI), RPMI was from Gibco (Grand Island, NY) and was used without antibiotics and buffered at pH 7.4, and brain heart infusion was from Difco (Detroit, MI).
10. R. Porat, unpublished data.
11. S. P. Eisenberg *et al.*, *Nature* **343**, 341 (1990); D. B. Carter *et al.*, *ibid.* **344**, 633 (1990); W. P. Arend, F. G. Joslin, R. J. Massoni, *J. Immunol.* **134**, 3868 (1985); P. Seckinger, J. W. Lowenthal, K. Williamson, J. M. Dayer, H. R. MacDonald, *ibid.* **139**, 1546 (1987).
12. A. V. Muchmore and J. M. Decker, *J. Biol. Chem.* **261**, 13404 (1987); *J. Immunol.* **138**, 2541 (1987); D. Pennica *et al.*, *Science* **236**, 83 (1987).
13. J. Mancilla *et al.*, *Cytokine* **1**, 95 (abstr.) (1989); D. T. Brody and S. K. Durum, *J. Immunol.* **143**, 1183 (1989).
14. W. C. Fanslow *et al.*, *Science* **248**, 739 (1990); S. K. Dower, personal communication.
15. J. D. Sipe, M. A. Johns, P. Ghezzi, G. Knapschaefer, *Adv. Exp. Med. Biol.* **243**, 193 (1988); M. A. Johns, J. D. Sipe, L. B. Melton, T. B. Strom, W. R. McCabe, *Infect. Immun.* **56**, 1593 (1988); B. H. Bjornson *et al.*, *ibid.*, p. 1602.
16. Statistical analyses were done on a Macintosh SE computer using StatView (BrainPower, Inc., Calabasas, CA). Data were subjected to analysis of variance, followed by Fisher's least significant difference test.
17. N. Savage *et al.*, *Cytokine* **1**, 23 (1989).


18. Supported by NIH grant AI 15614 and in part by the Sandoz Research Institute (to R.P.). We thank A. R. Shaw for providing the human recombinant IL-1β, and R. Neta, M. J. Barza, J. G. Cannon, D. R. Snydman, P. Shaw, A. R. Shaw, and D. Wallach for their help and advice.

2 May 1991; accepted 29 August 1991


# Primary Structure and Functional Expression of the $5HT_3$ Receptor, a Serotonin-Gated Ion Channel


ANDRES V. MARICQ, ANDREW S. PETERSON, ANTHONY J. BRAKE, RICHARD M. MYERS, DAVID JULIUS*



**The neurotransmitter serotonin (5HT) activates a variety of second messenger signaling systems and through them indirectly regulates the function of ion channels. Serotonin also activates ion channels directly, suggesting that it may also mediate rapid, excitatory responses. A complementary DNA clone containing the coding sequence of one of these rapidly responding channels, a $5HT_3$ subtype of the serotonin receptor, has been isolated by screening a neuroblastoma expression library for functional expression of serotonin-gated currents in *Xenopus* oocytes. The predicted protein product has many of the features shared by other members of the ligand-gated ion channel family. The pharmacological and electrophysiological characteristics of the cloned receptor are largely consistent with the properties of native $5HT_3$ receptors. Messenger RNA encoding this receptor is found in the brain, spinal cord, and heart. This receptor defines a new class of excitatory ligand-gated channels.**


SEROTONIN (5-HYDROXYTRYPTAMINE) is a biogenic amine that mediates a variety of physiological actions on distinct cell types, including neurons in the peripheral and central nervous system (CNS) of vertebrates (*1*). Serotonin exerts its actions by binding to distinct cell-surface receptors, pharmacologically classified into four major groups, $5HT_1$, $5HT_2$, $5HT_3$, and $5HT_4$. $5HT_1$, $5HT_2$, and $5HT_4$ receptors transduce extracellular signals by activating G proteins and mediate slow modulatory responses via second messenger signaling pathways (*2, 3*). In contrast, the $5HT_3$ receptor ($5HT_3R$) is a ligand-gated ion channel (*4, 5*), which when activated causes fast, depolarizing responses in neurons. Thus 5HT, like acetylcholine, γ-aminobutyric acid (GABA), and glutamate, activates both G protein–coupled receptors and ligand-gated ion channels.

The identification and characterization of $5HT_3Rs$ have been facilitated by the development of potent, highly selective drugs that bind to this receptor subtype (*6, 7*). $5HT_3R$ antagonists help prevent cytotoxic drug–evoked emesis, a common and severe side effect of most anticancer chemotherapeutic drug regimens (*8*). Because of their potential anxiolytic and antipsychotic properties, $5HT_3R$ antagonists are being explored as therapeutic agents for a variety of behavioral disorders (*9, 10*).


A. V. Maricq, A. J. Brake, D. Julius, Department of Pharmacology, University of California, San Francisco, CA 94143–0450.
A. Peterson, Department of Physiology, University of California, San Francisco, CA 94143–0444.
R. M. Myers, Departments of Physiology and Biochemistry and Biophysics, University of California, San Francisco, CA 94143–0444.

*To whom correspondence should be addressed.

Functional $5HT_3$Rs or binding sites for $5HT_3$R ligands have been identified in the enteric nervous system (*11*), on sympathetic, parasympathetic, and sensory nerve fibers, in the CNS (*12*), and on several mouse neuroblastoma cell lines (*13*). These receptors modulate intestinal contraction (*9*) and the transmission of pain sensation by sensory nerve fibers (*6*); however, the function of these receptors in the CNS remains obscure. Different properties of $5HT_3$Rs in these tissues suggest that there are multiple subtypes of the $5HT_3$R (*7, 9*).

Using expression cloning, we have now isolated a cDNA clone encoding a $5HT_3$ receptor ($5HT_3$R-A) from NCB-20 cells, a hybrid cell line derived from mouse neuroblastoma cells and Chinese hamster embryonic brain cells (*14*). The deduced amino acid sequence reveals that this receptor is a new member of the ligand-gated ion channel superfamily. RNA transcripts generated in vitro from this cDNA, when injected into *Xenopus* oocytes, are sufficient for functional expression of 5HT-gated ion channels. The resulting current has a divalent cation–mediated negative slope conductance that is reminiscent of that described for the NMDA subtype of glutamate receptor. The pattern of $5HT_3$R-A expression is consistent with $5HT_3$R antagonist binding sites in the brain and periphery.

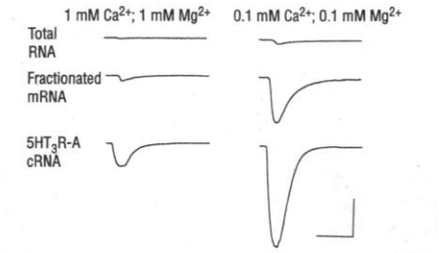


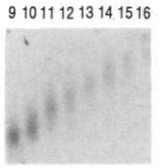


**Fig. 1.** Serotonin-dependent currents in *Xenopus* oocytes injected with mRNA from NCB-20 cells or RNA transcribed in vitro from p5HT3R-A. Collagenase-treated oocytes were single-electrode voltage clamped and held at −60 or −70 mV in Barth's solution. Downward deflection indicates inward (negative) current. Brief (1 to 5 s) bath application of 10 μM 5HT evoked reproducible inward currents. Top traces: total poly(A)$^+$ mRNA (50 ng), 6 days after injection; middle traces: mRNA from fraction 11 (25 ng), 5 days after injection; bottom traces: RNA transcribed in vitro from p5HT3R-A (0.4 ng), 1 day after injection. Calibration bars: 75 nA; 15 s (top two rows), 25 s (bottom row). (Inset) RNA blot analysis of poly(A)$^+$ NCB-20 mRNA size-fractionated by sucrose gradient centrifugation. Fractions were collected starting from the top of the gradient. $^{32}$P-labeled oligo(dT) was used as the probe. Size standards (in kilobases) are on the left.

NCB-20 cells express relatively large amounts of the $5HT_3$R (*13*). We therefore injected polyadenylated [poly(A)$^+$] mRNA from NCB-20 cells into *Xenopus* oocytes and tested for the presence of 5HT-gated currents (*15, 16*). The oocytes responded to bath application of 5HT with a rapidly developing, inward current (Fig. 1). This current was blocked by selective antagonists of $5HT_3$Rs, desensitized rapidly in the continued presence of agonist, and increased in amplitude upon decreasing the concentration of divalent cations in the external solution (Fig. 1). To increase the amplitude of these responses, we minimized desensitization by using a small perfusion chamber in which solutions could be exchanged rapidly, increased current amplitude by lowering the concentrations of divalent cations in the perfusate, and size-fractionated the mRNA to enrich for an active component. After fractionation of poly(A)$^+$ mRNA by sucrose density gradient centrifugation, 5HT-evoked current was observed only with mRNA from two fractions (*9* and *10*) containing mRNA ranging in size from 2 to 2.5 kb (Fig. 1).

We constructed a cDNA library in an RNA expression vector (pCDM6XL) from the two positive mRNA fractions (*17*). RNA transcripts prepared from five pools, each representing ~100,000 independent clones, were injected separately into *Xenopus* oocytes. Currents evoked by 5HT were observed with transcripts from one of these pools, and the current amplitude increased when the concentration of external divalent cations was reduced from 1.0 to 0.2 mM. Serial dilution of the positive pool yielded a single clone, p5HT3R-A. Oocytes injected with transcripts produced from this clone responded to 5HT with a large, rapidly developing, inward current that also increased in amplitude when the concentration of external divalent cations was reduced (Fig. 1). 5HT application did not produce the long-lasting oscillatory $Cl^-$ current characteristically elicited by activation of G

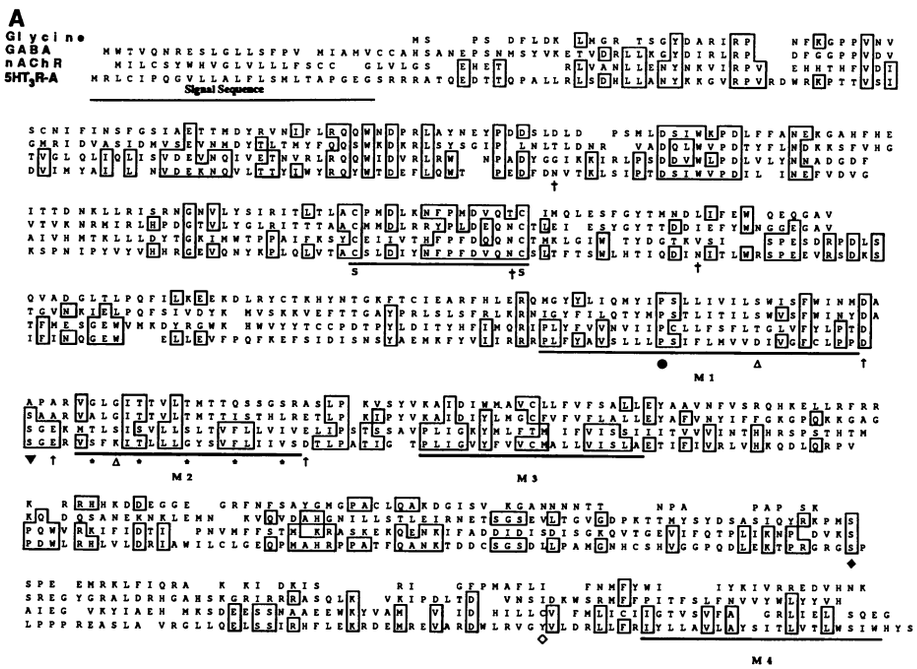


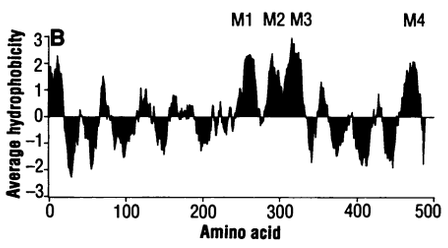


**Fig. 2.** Amino acid sequence and hydrophobicity profile for mouse $5HT_3$R-A. The nucleotide sequence has been deposited in GenBank (accession number M74425). (**A**) The amino acid sequence of $5HT_3$R-A and its alignment with other members of the ligand-gated channel superfamily. The amino acid sequences were aligned with the GENALIGN program (UCSF Computing Center) and identities are indicated by the boxed regions. Four hydrophobic regions were assigned on the basis of hydrophobicity analysis (M1-M4). S-S, Cys-Cys loop; †, potential *N*-glycosylation sites; ▼, potential casein kinase phosphorylation site; ◇, potential protein kinase A phosphorylation site; ◆, potential tyrosine phosphorylation site. Arrows, conserved cytoplasmic and extracellular charges (*39*); ●, a conserved proline; *, residues believed to line the channel pore (*37*); △, charged residues in M1 and M2. Abbreviations for the amino acid residues are A, Ala; C, Cys; D, Asp; E, Glu; F, Phe; G, Gly; H, His; I, Ile; K, Lys; L, Leu; M, Met; N, Asn; P, Pro; Q, Gln; R, Arg; S, Ser; T, Thr; V, Val; W, Trp; and Y, Tyr. (**B**) Hydrophobicity profile of $5HT_3$R-A drawn by using the Kyte-Doolittle algorithm with a window setting of 15 (*39*).

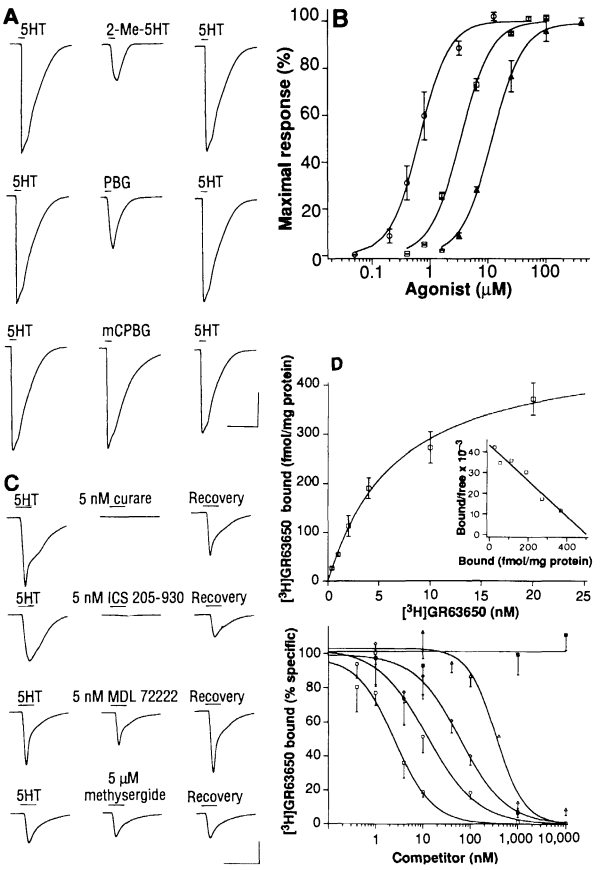


**Fig. 3.** Pharmacological characterization of cloned $5HT_3Rs$ expressed in *Xenopus* oocytes. (**A**) Agonist profile. Oocytes were voltage-clamped (−70 mV) 1 to 2 days after injection of 0.4 ng of in vitro transcript from p5HT3R-A while bathed in Barth's solution. Drugs (10 μm) were applied for 5 s as follows: 5HT; 90-s recovery period; 2Me-5HT, PBG, or mCPBG; 90-s recovery period; 5HT. All records were obtained from one oocyte. Calibration bars: 200 nA, 25 s. (**B**) Dose-response curves for (□) 5HT, (△) 2Me-5HT, and (○) mCPBG. Recordings were performed as in (A). Each point (±SEM) represents the average value from three oocytes. Dose-response curves were fitted to the logistic equation: $I = I_{max} \times \{(dose)^n/[EC_{50}^n + (dose)^n]\}$. The mean $EC_{50}$ and Hill coefficient values (SD) were 3.4 μM (0.38), 1.65 (0.14); 12.5 μM (2.7), 1.69 (0.53); and 0.7 μM (0.25), 1.81 (0.26) for 5HT, 2Me-5HT, and mCPBG, respectively. (**C**) Antagonist profile. Oocytes were voltage-clamped at −70 mV and bathed for 30 s in a solution containing one of the antagonists. 5HT (10 μM) was then applied with the antagonist for 5 s. The mean percent of control current (±SD) in the presence of ICS 205-930, MDL 72222, curare, and methysergide was 2.1 ± 1.4, 57 ± 4.4, 1.1 ± 1.2, and 72 ± 7.6, respectively. The current recovered with a time course that depended on the previously applied antagonist. Partial recovery current traces recorded 9 min after the washout of the antagonist ICS 205-930 are shown. Recovery time for all other antagonists was 200 s. Calibration bars: 200 nA, 10 s. (**D**) (Top) Binding of [$^3$H]GR63650 to membranes from COS-1 cells expressing $5HT_3R$-A. The results are derived from duplicate measurements of binding in the presence or absence of the $5HT_3R$ antagonist zacopride. Specific binding represented 68 to 78% of the total binding. (Inset) Scatchard transformation of the data. (Bottom) Competition by various drugs for [$^3$H]GR63650 binding to $5HT_3R$-A expressed in COS-1 cells. Membranes were incubated in the presence of 2 nM [$^3$H]GR63650 and varying concentrations of competitor. Points represent means of duplicate measurements. □, ICS 205-930; ○, *d*-tubocurarine; ◇, MDL 72222; △, 5HT; ■, methysergide.

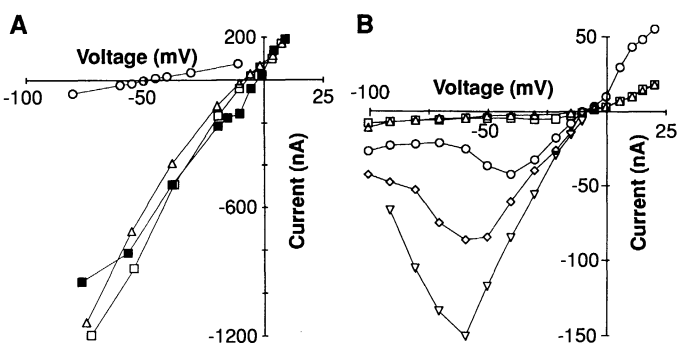


**Fig. 4.** Electrophysiological characterization of $5HT_3R$-A. (**A**) Reversal potential measurements of the 5HT-dependent conductance expressed from in vitro transcripts of p5HT3R-A. Oocytes were injected with 0.4 ng of cRNA and voltage-clamp recordings made on the following day. *I-V* relations were recorded from an oocyte bathed in solutions that contained 0.1 mM $Ca^{2+}$, nominally 0 mM $Mg^{2+}$, 2 mM Hepes (pH 7.4), and either 100 mM $Na^+$, 100 mM $K^+$, or 100 mM tris (pH 7.1). The order of solution changes was (□) $Na^+$, (△) $K^+$, (○) tris, and (■) return to $Na^+$. Measurements within the same oocyte were reproducible. Reversal potentials ($E_{rev}$) were estimated by fitting a second order polynomial to the data points on either side of the zero-current value. $E_{rev}$ was calculated from measurements in three different oocytes. The calculated $E_{rev}$ was −7.1, −8.3, −50.1, and −2.5 mV, for $Na^+$, $K^+$, tris, and return to $Na^+$, respectively. Similar results were obtained from two additional oocytes. (**B**) *I-V* relations of the 5HT-dependent conductance. Same protocol as in (A). The membrane current was elicited by 5-s applications of 2 μM 5HT. The external solution containing 100 mM $Na^+$, nominally 0 mM $Mg^{2+}$, and either (▽) 0.1, (◇) 0.3, (○) 1.0, (□) 3.0, or (△) 10.0 mM $Ca^{2+}$. Measurements were separated by recovery periods of 90 to 120 s. All measurements were from one representative oocyte. Similar results were obtained from six additional oocytes.

protein–coupled receptors such as the $5HT_{1C}$ and $5HT_2$ subtypes (*3*). The current responded with little delay, exhibited a monotonic decrease with time, and was stable to repeated applications of 5HT for several hours.

Sequence analysis of p5HT3R-A shows that it encodes a member of the ligand-gated ion channel family. The 2131-bp cDNA insert of p5HT3R-A has one large open reading frame that extends from an ATG at position 1 (preceded by 60 bp of 5′ untranslated sequence) to a termination codon at nucleotide 1462 (Fig. 2A). The cDNA contains a consensus poly(A) addition site (AATAAA) (*18*) followed by a poly(A) tail. The predicted protein is 487 amino acids long with a molecular weight of 55,966. Sequence comparisons place the $5HT_3R$-A in the superfamily of ligand-gated ion channels (*19, 20*) (Fig. 2). The receptor exhibits sequence similarity to the α subunit of the *Torpedo californica* nicotinic acetylcholine receptor (27% identity), the β1 subunit of the bovine $GABA_A$ receptor (22%), and the 48K subunit of the rat glycine receptor (22%) (Fig. 2A). In addition, many of the characteristic features of this superfamily are found in the $5HT_3R$-A cDNA. Thus, hydrophobicity analysis of the $5HT_3R$-A predicts a topological organization in which the protein contains four hydrophobic transmembrane regions (M1 through M4), a large $NH_2$-terminal extracellular domain, and a long cytoplasmic loop connecting M3 to M4 (Fig. 2B). In addition, the $NH_2$-terminal extracellular domain contains a signature feature of this family, the Cys-Cys loop (Cys . . . Pro Asp . . . Cys), in which two invariant cysteines, spaced 14 residues apart, are thought to participate in the formation of a disulfide bond (*19*).

The generation of currents with a single clone demonstrates that functional, homomeric $5HT_3Rs$ can be formed in the oocyte. Other members of the ligand-gated ion channel family are pentameric membrane proteins with between two and four homologous subunits (*21, 22*). Single subunits from some members of this family can form functional homomeric receptors, but they generally lack some properties of the native, multisubunit receptors (*23*). By analogy the native $5HT_3R$ is also likely to be composed of several different subunits.

To characterize $5HT_3R$-A, we used three selective agonists for $5HT_3Rs$ (*7*): 2-methyl-5-hydroxytryptamine (2-Me-5HT), 1-phenyl-biguanide (PBG), and 1-(*m*-chlorophenyl)-biguanide (mCPBG) (*24*). Oocytes injected with RNA transcripts from p5HT3R-A responded with a rapidly developing, inward current to all three ago-

nists (Fig. 3A). The time courses of onset and decay of these currents were similar, and the effect of each agonist was fully reversible. A dose-response analysis established the order of potency as mCPBG > 5HT > 2-Me-5HT (Fig. 3B). The Hill coefficients obtained from the logistic equation fit of the dose-response data were similar (1.81, 1.65, 1.69), a result suggesting that activation of the $5HT_3$R-A requires the binding of more than one ligand molecule. Prolonged application of agonist resulted in a desensitized state that could last for minutes, especially with mCPBG. Although desensitization may cause the true Hill coefficient to be underestimated, the calculated Hill coefficients are in general agreement with those obtained from electrophysiological recordings of neuroblastoma cells (*25–27*) and cultured hippocampal neurons (*4*).

We tested the effects of $5HT_3$R antagonists, which distinguish among subtypes of the $5HT_3$Rs (*2*), on 5HT-activated currents. Both ICS 205-930 and MDL 72222 reversibly inhibited 5HT-evoked currents (Fig. 3C). Superfusion of oocytes with 5 nM ICS 205-930 almost completely blocked the current response to 5HT. As in hippocampal neurons and neuroblastoma cells (*4*), the effects of ICS 205-930 were only slowly reversible, and partial recovery was seen after 10 min. In contrast to the lack of effect of MDL 72222 on $5HT_3$Rs in enteric neurons (*9*), this drug reversibly antagonized the 5HT-evoked current in oocytes. Methysergide, an antagonist of G protein–coupled 5HT receptors (*22*), did not appreciably inhibit the current. As in neuroblastoma cells (*4*), *d*-tubocurarine (curare) reversibly blocked the $5HT_3$R-A receptor at nanomolar concentrations. Although curare, a competitive antagonist of nAChRs, binds to the $5HT_3$R with a tenfold greater affinity than it does to the nAChR (*4*), application of 10 μM acetylcholine to oocytes expressing the $5HT_3$R-A did not produce detectable membrane current.

In the continued presence of 5HT, the current passing through the $5HT_3$R-A channel declined rapidly, decaying to zero within seconds to tens of seconds. Moreover, after a long exposure to 5HT, a recovery period was required before test pulses of 5HT could elicit a maximal response. This process of desensitization is characteristic of most ligand-gated channels, including the $5HT_3$R (*4, 27–29*).

We also carried out radioligand binding studies of the $5HT_3$R-A (*30*) with membranes prepared from COS-1 cells that had been transiently transfected with p5HT3R-A (Fig. 3D). Membranes from such cells specifically bound the $5HT_3$R selective antagonist [$^3$H]GR63650 with a dissociation constant ($K_d$) of 7.1 (±1.2 SD) nM, and a Hill coefficient of 0.95 (±0.15). COS-1 cells transfected with the plasmid vector alone showed no specific binding. Parallel experiments on membranes prepared from NCB-20 cells showed a $K_d$ of 8.0 (±1.5) nM and a Hill coefficient of 1.07 (±0.15). We examined whether other antagonists of the $5HT_3$R could compete for [$^3$H]GR63650 binding sites on the transfected COS-1 cells (Fig. 3D). The drugs tested competed for binding with the same order of potency (ICS 205-930 > curare > MDL 72222 > 5HT > methysergide) and with similar $K_i$ values (*30*) as for [$^3$H]GR63650 binding to NCB-20 membranes (*31*) or rat cortical tissue (*12*). Thus, the $5HT_3$R-A expressed from the cloned cDNA has the drug binding sites that are characteristic of native $5HT_3$Rs.

The native $5HT_3$R is a cation-specific, but otherwise relatively nonselective, ion channel (*32*). Are these properties conserved in the homo-oligomeric $5HT_3$R-A? Current-voltage (*I-V*) relations from oocytes expressing the $5HT_3$R-A revealed a reversal potential close to 0 mV (Fig. 4A). When all external $Na^+$ was replaced by the large organic cation tris, the reversal potential shifted to −50 mV and the amplitude of the current decreased. These findings suggest that the channel is primarily cation-selective but discriminates poorly, allowing the passage of even large cations. When all external $Na^+$ was replaced by $K^+$, the estimated reversal potential only shifted from −7.1 to −8.3 mV, suggesting that $Na^+$ and $K^+$ have approximately the same permeability through the $5HT_3$R-A channel. The effects of ion substitution on the reversal potential were fully reversible (Fig. 4A) and similar to the properties of $5HT_3$Rs in neuroblastoma cells (*25, 32*).

Calcium ions reduce the macroscopic conductance of the $5HT_3$R without otherwise affecting the *I-V* relations (*25, 33*). In this regard, the $5HT_3$R-A behaves differently from the native $5HT_3$R (Fig. 4B). *I-V* relations from oocytes bathed in solutions containing $Ca^{2+}$ from 0.1 to 1.0 mM have a region of negative-slope conductance where the current increases in amplitude as the cell is progressively depolarized; with further depolarization the current decreases until it reaches zero at the reversal potential. At all voltages, the current amplitude decreased with increases in the external $Ca^{2+}$ concentration; when the $Ca^{2+}$ was raised to 3.0 or 10.0 mM, the inward current was nearly abolished and the region of negative slope conductance was barely discernible (Fig. 4B). In contrast, there was little effect of $Ca^{2+}$ on the estimated reversal potential, suggesting that $Ca^{2+}$ ions have a voltage-dependent blocking action on the 5HT-gated current. When the concentration of external $Mg^{2+}$ was varied, a region of negative slope conductance was also apparent: The amplitude of the current decreased with increases in $Mg^{2+}$ concentration, and variation of the external $Mg^{2+}$ concentration did not appreciably alter the reversal potential. Negative slope conductance is a feature of several voltage-dependent channels; however, among ligand-gated channels, it has been only found for the *N*-methyl-D-aspartate (NMDA) subtype of glutamate channel. The negative slope conductance of the NMDA channel has been attributed to a voltage-dependent $Mg^{2+}$ block of the channel (*34*). In contrast to the NMDA receptor, either $Ca^{2+}$ or $Mg^{2+}$ can have a voltage-dependent blocking effect on the $5HT_3$R-A channel.

We examined the expression of $5HT_3$R-A mRNA in various tissues (Fig. 5) and compared this to the known distribution of $5HT_3$Rs. Although a 2.2-kb RNA species was readily detectable by RNA blotting with poly(A)$^+$ RNA prepared from neuroblastoma cell lines (Fig. 5A), no signal was evident from RNA prepared from a variety of tissues. Therefore, we used the polymerase chain reaction (PCR) (*35*) to amplify $5HT_3$R-A sequences from these tissues. A

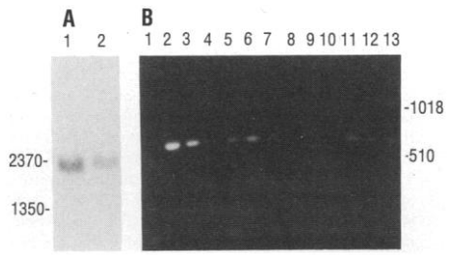


**Fig. 5.** Tissue distribution of $5HT_3$R-A mRNA. (**A**) 1 μg of poly(A)$^+$ RNA from (lane 1) NCB-20 or (lane 2) NIE-115 cells was electrophoresed on a 0.8% formaldehyde agarose gel, transferred to nylon membrane, and hybridized at 65° with $^{32}$P-labeled p5HT3R-A. The blot was washed at 65° in 0.1 × SSC. (**B**) PCR reaction products were electrophoresed on a 1.2% agarose gel and nucleic acids were visualized by ethidium-bromide fluorescence. Sources of the RNA for the PCR templates were (lane 1) no template added, (lane 2) N1E-115, (lane 3) NCB-20, (lane 4) lung, (lane 5) brainstem, (lane 6) cortex, (lane 7) liver, (lane 8) spleen, (lane 9) intestine, (lane 10) cerebellum, (lane 11) midbrain, (lane 12) spinal cord, (lane 13) heart. The template for each of the reactions consisted of 0.1% of an oligo-dT–primed first strand cDNA reaction, synthesized with 0.5 μg of poly(A)$^+$ RNA from NCB-20 and N1E-115 cells or 5 μg of total RNA from each of the mouse tissues. 40 cycles of PCR (1 min at 95°; 30 s at 65°; 2 min at 72°) were performed with oligonucleotide primers corresponding to positions 84–114 and 682–712 of the $5HT_3$R-A sequence.

single PCR product of the predicted size (0.6 kb) was identified in mouse cortex, brainstem, midbrain, spinal cord, and heart. No PCR products were seen in samples from cerebellum, liver, lung, spleen, or intestine (Fig. 5B). The distribution of message is consistent with ligand binding studies (*9, 12*) except for the absence of signal from the intestine. The $5HT_3R$ in the intestine may be a distinct subtype encoded by a separate gene.

The channel pore of the nAChR is thought to be formed by the contribution of a transmembrane α helix from each of the five subunits (*21, 36*). In this view of the nAChR, the M2 helix from each subunit lines the pore (*37*), with possible contributions from the M1 helix (*38*). Within the M1, M2, and M3 transmembrane regions of the $5HT_3R$-A and the mouse muscle nAChR, residues that have important structural or functional roles in nAChRs are conserved. Negatively charged residues, immediately $NH_2$-terminal and immediately COOH-terminal to M2, are found in both the $5HT_3R$-A and the nAChRs. These residues have been proposed to participate in the formation of ion-attracting vestibules at the entrances to the channel; site-directed mutagenesis of these residues dramatically affects both the conductance and the rectification of the nicotinic receptors (*39*). The lining of the pore is composed of side chains from residues that line one face of the M2 α helix (*37*). These residues, at every fourth position, would interact most directly with permeating ions. The extracellular portion of the nAChR pore is lined by hydrophobic residues, the middle is lined by short chain amino acids, and the intracellular portion is lined by amino acids with side chains containing hydroxyl groups. Similar residues in the $5HT_3R$-A occupy these positions within the predicted M2 helix (Fig. 2).

Among these similarities are two striking differences. The M1 region of the $5HT_3R$-A has a negatively charged aspartate at position 264, near the cytoplasmic side of the putative M1 α helix. Similarly, there is a positively charged lysine in M2, at position 281, near what would be the cytoplasmic end of that α helix. The presence of these charged residues within the membrane is energetically unfavorable and reduces the probability that these regions exist as isolated transmembrane helices; however, as these charged residues are in adjacent helices they may interact and neutralize each other's charge, likely affecting the conductance and gating of the pore. The charged amino acids could also play a role in the divalent cation–mediated negative slope conductance in $5HT_3R$-A but not in the nAChR (*21*). An explanation for this negative slope conductance, which we observe in oocytes but that, is not seen in neurons (*25, 27, 29, 32*), is that additional subunits may be present in native $5HT_3Rs$. Differences in conductance states between intestine (14 and 19 pS) (*5*) and neuroblastoma cells (0.3 to 0.6 pS by noise analysis) (*25, 32*) points to the existence of multiple $5HT_3R$ molecular species.

Like the NMDA receptor, the $5HT_3R$-A channel is modulated by both external $Ca^{2+}$ and $Mg^{2+}$ and may be useful for the study of divalent modulation of channel conductance. The cloning and single-channel characterization of additional members of the $5HT_3R$ family will help to elucidate the function of this excitatory receptor in the nervous system.

## REFERENCES AND NOTES


1. M. M. Rapport, A. A. Green, I. H. Page, *J. Biol. Chem.* **176**, 1243 (1948); J. H. Gaddum and Z. P. Picarelli, *Br. J. Pharmacol. Chemother.* **12**, 323 (1957); P. J. M. Tutton and D. H. Barkla, *Anticancer Res.* 7, 1 (1987); A. Frazer, S. Maayani, B. Wolfe, *Annu. Rev. Pharmacol. Toxicol.* **30**, 307 (1990).
2. P. B. Bradley *et al.*, *Neuropharmacology* **25**, 563 (1986).
3. S. J. Peroutka, *Annu. Rev. Neurosci.* **11**, 45 (1988); D. J. Julius *ibid.* **14**, 335 (1991).
4. J. L. Yakel and M. B. Jackson, *Neuron* **1**, 615 (1988).
5. V. Derkach, A. Suprenant, R. North, *Nature* **339**, 706 (1989).
6. B. P. Richardson, G. Engel, P. Donatsch, P. A. Stadler, *ibid.* **316**, 126 (1985).
7. B. P. Richardson and G. Engel, *Trends Neurosci.* **9**, 424 (1986).
8. K. Bunce, M. Tyers, P. Beranek, *Trends Pharmacol. Sci.* **12**, 46 (1991).
9. B. P. Richardson and K.-H. Bucheit, in *Neuronal Serotonin*, N. N. Osborne and M. Hamon, Eds. (Wiley, New York, 1988), pp. 465–506.
10. B. Costall, R. J. Naylor, M. B. Tyers, *Rev. Neurosci.* **2**, 41 (1988).
11. J. H. Gaddum and Z. P. Picarelli, *Br. J. Pharmacol. Chemother.* **12**, 323 (1957); T. Branchek, M. Kates, M. D. Gershon, *Brain Res.* **324**, 107 (1984); J. C. Gordon, D. S. Barefoot, N. S. Sarbin, L. M. Pinkus, *J. Pharmacol. Exp. Ther.* **251**, 962 (1989).
12. G. J. Kilpatrick, B. J. Jones, M. B. Tyers, *Nature* **330**, 746 (1987); D. Hoyer, C. Waeber, A. Karpf, H. Neijt, J. M. Palacios, *Naunyn-Schmiedebergs Arch. Pharmakol.* **340**, 396 (1989); M. Hamon *et al.*, *Eur. J. Pharmacol.* **164**, 315 (1989); C. M. Milburn and S. J. Peroutka, *J. Neurochem.* **52**, 1787 (1989).
13. D. Hoyer and H. C. Neijt, *Eur. J. Pharmacol.* **143**, 291 (1987); D. Hoyer and H. D. Neijt, *Mol. Pharmacol.* **33**, 303 (1988); R. M. McKernan, K. Quirk, R. G. Jackson, C. I. Ragan, *J. Neurochem.* **54**, 924 (1990).
14. J. Minna, J. Yavelow, H. C. Coon, *Genetics (Suppl.)* **79**, 373 (1975).
15. NCB-20 cells were grown as described (*14*), and total cellular RNA was isolated by the guanidine thiocyanate method [G. Cathala *et al.*, *DNA* **2**, 329 (1983)]. The poly(A)$^+$ mRNA was purified and size-fractionated on a 5% to 25% (w/v) sucrose gradient. [D. Julius, A. B. MacDermott, R. Axel, T. M. Jessell, *Science* **241**, 558 (1988)].
16. *Xenopus* oocytes were prepared as described [C. J. Marcus-Sekura and M. J. M. Hitchcock, in *Guide to Molecular Cloning Techniques*, S. L. Berger and A. R. Kimmel, Eds. (Academic Press, New York, 1987), pp. 284–288]. Voltage-clamp recording was performed with a single electrode and the Axoclamp II in dSEVC mode (Axon Inst. Co.). The recording chamber was 3 mm by 1.5 mm by 3 mm and perfusate flow rate was regulated at 5 to 15 ml/min. Electrode resistances ranged from 0.5 to 1.0 megohms when filled with either 3 M KCl or 1.5 M KCl, 0.25 M EGTA. Current and voltage records were digitized at 2 to 20 Hz and stored on a Macintosh computer.
17. A directional cDNA library was constructed from 4 μg of NCB-20 poly(A)$^+$-selected mRNA as described [A. Aruffo and B. Seed, *Proc. Natl. Acad. Sci. U.S.A.* **84**, 8573 (1987)]. cDNA was synthesized with a Not I oligo-dT primer and inserted into pCDM6XL, which was constructed from pCDM by incorporating a short region of the 5′ untranslated region of *Xenopus* β-globin immediately downstream of the SP6 promoter. DNA templates were linearized with Not I and transcribed with SP6 RNA polymerase. Clone p5HT3R-A was completely sequenced on both strands by standard methods [F. Sanger, S. Nicklen, A. R. Coulson, *Proc. Natl. Acad. Sci. U.S.A.* **74**, 5463 (1977)].
18. J. Nevins, *Annu. Rev. Biochem.* **52**, 441 (1983).
19. G. Grenningloh *et al.*, *Nature* **330**, 25 (1987); E. A. Barnard, M. G. Darlison, P. Seeburg, *Trends Neurosci.* **10**, 502 (1987); H. Betz, *Neuron* **5**, 383 (1990); P. R. Schofield *et al.*, *Nature* **328**, 221 (1987); G. Grenningloh *et al.*, *ibid.*, p. 215; G. Grenningloh *et al.*, *Neuron* **4**, 963 (1990).
20. M. Hollmann, A. O'Shea-Greenfield, S. W. Rogers, S. Heinemann, *Nature* **342**, 643 (1989).
21. S. Numa, *Harvey Lect.* **83**, 121 (1989).
22. D. Langosch, L. Thomas, H. Betz, *Proc. Natl. Acad. Sci. U.S.A.* **85**, 7394 (1988); R. W. Olsen and A. J. Tobin, *FASEB J.* **4**, 1469 (1990).
23. M. Mishina *et al.*, *Nature* **321**, 406 (1986); L. A. C. Blair, E. D. Levitan, J. Marshall, V. Dionne, E. A. Barnard, *Science* **242**, 577 (1988); V. Schmieden, G. Grenningloh, P. Schofield, H. Betz, *EMBO J.* **8**, 695 (1989); S. Couturier *et al.*, *Neuron* **6**, 847 (1990).
24. G. J. Kilpatrick, A. Butler, J. Burridge, A. W. Oxford, *Eur. J. Pharmacol.* **182**, 193 (1990).
25. J. J. Lambert, J. A. Peters, T. G. Hales, J. Dempster, *Br. J. Pharmacol.* **97**, 27 (1989).
26. H. C. Neijt, I. J. te Duits, H. P. M. Vijverberg, *Neuropharmacology* **27**, 301 (1988).
27. H. C. Neijt, J. J. Plomp, H. P. M. Vijverberg, *J. Physiol. (London)* **411**, 257 (1989).
28. B. Katz and S. Thesleff, *ibid.* **138**, 63 (1957).
29. X. M. Shao, J. L. Yakel, M. B. Jackson, *J. Neurophysiol.* **65**, 630 (1991).
30. COS-1 cells were transfected with p5HT3R-A (10 μg per $10^7$ cells) in phosphate buffered saline (PBS) with a Bio-Rad Gene Pulsar set at 300 V and 960 μF. After 48 to 72 hours of growth, cells were harvested, washed with PBS, and homogenized in 5 volumes of 0.32 M sucrose, 50 mM tris-Cl, pH 7.5, 1 mM EDTA containing the protease inhibitors aprotinin (10 μg/ml), leupeptin (0.5 μg/ml), pepstatin (0.75 μg/ml), benzamidine (0.1 mM), phenylmethylsulfonyl fluoride (0.5 mM), and *trans*-epoxysuccinyl-L-leucylamido-(4-guanidino)-butane (1 μM). After centrifugation at 750*g* for 10 min, the supernatant fraction was recentrifuged at 100,000*g* for 45 min. The resulting pellet was resuspended to a protein concentration of approximately 5 mg/ml in 50 mM tris-Cl, 1 mM EDTA, pH 7.5 containing the same protease inhibitors described above. For ligand binding experiments, membranes containing 100 to 300 μg of protein were incubated in a total volume of 0.5 ml of 50 mM tris, 1 mM EDTA, pH 7.5 with the indicated concentrations of [$^3$H]GR63650 (New England Nuclear, 64 Ci/mM) at 37° C for 30 min. The reactions were terminated by addition of 5 ml of ice-cold 50 mM tris-Cl, pH 7.5. Membranes were collected by rapid filtration through Whatman GF/B filters and washed twice with 5 ml of the same buffer. Radioactivity was determined by liquid scintillation spectroscopy. Nonspecific binding was determined in the presence of 10 μM zacopride. Data were analyzed by nonlinear curve fitting to the Hill equation with the program Enzfitter (Biosoft). Values (±SD) for $K_i$ and Hill coefficients were, respectively, for ICS 205-930, 2.1 ± 0.4 nM and 1.07 ± 0.25; for curare, 8.8 ± 2.3 nM and 0.84 ± 0.16; for MDL 72222, 88 ± 35 nM and 0.61 ± 0.14; for 5HT, 270 ± 50 nM and 1.92 ± 0.55; and for methysergide, $K_i$ > 10,000 nM.
31. R. M. McKernan *et al.*, *J. Biol. Chem.* **265**, 13572 (1990).

32. J. Yang, *J. Gen. Physiol.* **96**, 1177 (1990).
33. J. A. Peters, T. G. Hales, J. J. Lambert, *Eur. J. Pharmacol.* **151**, 491 (1988).
34. L. Nowak, P. Bregestovski, P. Ascher, A. Herbert, A. Prochiantz, *Nature* **307**, 462 (1984).
35. K. Mullis *et al.*, *Cold Spring Harb. Symp. Quant. Biol.* **51**, 263 (1986).
36. M. Montal, *FASEB J.* **4**, 2623 (1990); J.-P. Changeux, *Trends Pharmacol. Sci.* (1990).
37. R. J. Leonard, C. G. Labarca, P. Charnet, N. Davidson, H. A. Lester, *Science* **242**, 1578 (1988); P. Charnet *et al.*, *Neuron* **4**, 87 (1990).
38. J. A. Dani, *Trends Neurosci.* **12**, 125 (1989).
39. K. Imoto *et al.*, *Nature* **324**, 670 (1986); K. Imoto *et al.*, *ibid.* **335**, 645 (1988).
40. J. Kyte and R. Doolittle, *J. Mol. Biol.* **157**, 105 (1982).

41. We thank H. Bourne, L. Jan, J. Lansman, R. Nicoll, and Z. Hall for comments and suggestions on the manuscript; N. Patil, P. Garcia, and U. Garuda for helpful discussions and expert advice; and C. S. Yost, B. Richardson, and J. Parks for gifts of pCDM6XL, ICS 205–930, and zacopride, respectively. Supported by a NIH postdoctoral training grant (A.V.M.), a grant from the National Institutes of Health (GM44298) (D.J.), a NSF Presidential Young Investigator Award (D.J.), the Jane Coffin Childs Memorial Fund for Medical Research (A.S.P.), and the Wills Foundation (A.S.P., and R.M.M.). D.J. thanks the PEW Memorial Trust and the McKnight Foundation for Neuroscience for support.

30 May 1991; accepted 6 August 1991

# Reversible Inhibition of Tomato Fruit Senescence by Antisense RNA

PAUL W. OELLER, LU MIN-WONG, LOVERINE P. TAYLOR,*
DEBORAH A. PIKE,† ATHANASIOS THEOLOGIS‡

**Ethylene controls fruit ripening. Expression of antisense RNA to the rate-limiting enzyme in the biosynthetic pathway of ethylene, 1-aminocyclopropane-1-carboxylate synthase, inhibits fruit ripening in tomato plants. Administration of exogenous ethylene or propylene reverses the inhibitory effect. This result demonstrates that ethylene is the trigger and not the by-product of ripening and raises the prospect that the life-span of plant tissues can be extended, thereby preventing spoilage.**

IN PLANTS, RIPENING OF A FRUIT IS the prelude to senescence, the final phase of development and differentiation (*1, 2*). During ripening, climacteric fruits, such as tomato and banana, undergo marked changes in composition and texture and have a burst of respiration (climacteric rise) with a concomitant increase in ethylene ($C_2H_4$) production (*1, 3*). Climacteric fruits can be induced to ripen by treatment with $C_2H_4$ at concentrations above 0.1 μl of $C_2H_4$ per liter of air. Once ripening is initiated, the endogenous $C_2H_4$ production rises autocatalytically (*4*). Ethylene affects gene transcription in a variety of tissues (*5*), and physiological evidence indicates that $C_2H_4$ is the natural ripening hormone (*1, 6,* 7). We now use antisense RNA to inactivate the rate-limiting enzyme in the $C_2H_4$ biosynthetic pathway and show that $C_2H_4$ triggers ripening and senescence of tomato (*Lycopersicon esculentum*) fruit.

The rate-limiting step in the synthesis of $C_2H_4$ is the conversion of S-adenosylmethionine to 1-aminocyclopropane-1-carboxylic acid (ACC), the immediate precursor of $C_2H_4$, a process that is catalyzed by the enzyme ACC synthase (*4, 8*). Induction of $C_2H_4$ production requires de novo synthesis of this enzyme (*8*). ACC synthase is encoded in tomato by a divergent multigene family, two members of which are expressed during fruit ripening (*9*). Full-length cDNAs from the two genes, *LE-ACC2* and *LE-ACC4*, have been isolated and structurally characterized (*9*).

We expressed antisense RNA derived from the tACC2 cDNA of the *LE-ACC2* gene constitutively in transgenic plants using the cauliflower mosaic virus (CaMV) 35*S* promoter (Fig. 1A). Thirty-four independent transgenic tomato plants were obtained, and three of them, A11.1, A11.4, and A2, showed a marked inhibition in $C_2H_4$ production and delay in the onset of fruit ripening. The strongest phenotype was observed with fruits from the A11.1 transformant, which was chosen for further analysis. All of the experiments reported here have been carried out with homozygous A11.1 fruits from the second (R1) or third (R2) generation of transgenic plants. Southern (DNA) blot analysis showed that A11.1 plants from the R1 generation (Fig. 1B) contained an additional 1.7-kb DNA fragment that segregated as a single locus (3:1 ratio). Comparison of the hybridization intensities between the endogenous single-copy *LE-ACC2* synthase gene (*9*) and the antisense gene indicates the presence of ten antisense insertions per plant (Fig. 1B).

Control fruits kept in air begin to produce $C_2H_4$ 48 to 50 days after pollination, then undergo a respiratory burst (*10*), and fully ripen after ten more days (Figs. 2A and 3). Ethylene production was inhibited by 99.5% in antisense fruits, which fail to ripen (Fig. 2A). The basal level of $C_2H_4$ evolution in antisense fruits is below 0.1 nl of $C_2H_4$ per gram of fruit mass per hour. The red coloration resulting from chlorophyll degradation and lycopene biosynthesis is also inhibited in antisense fruits (*11*). A progressive loss of chlorophyll from antisense fruits is seen 10 to 20 days later than the loss is seen in the control fruits, resulting in a yellow color. Antisense fruits kept in air or on the plants for 90 to 120 days eventually develop an orange color but never turn red and soft (*12*) or develop an aroma. Antisense fruits in air do not show the respiratory

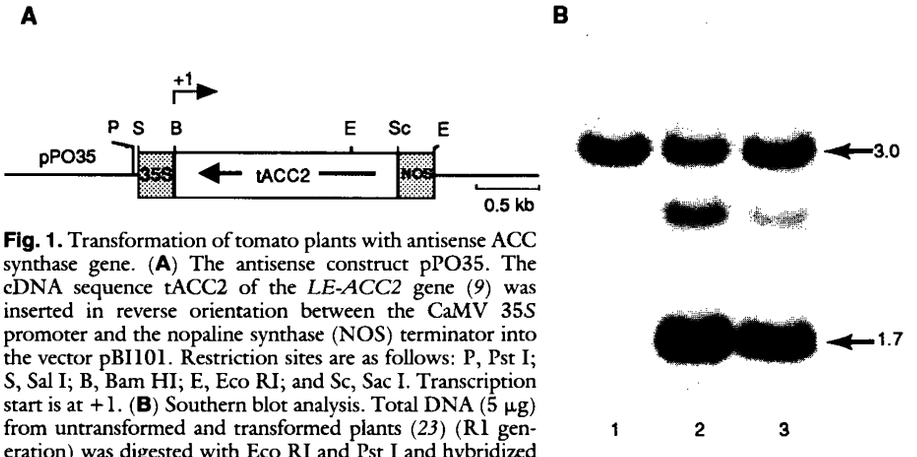


**Fig. 1.** Transformation of tomato plants with antisense ACC synthase gene. (**A**) The antisense construct pPO35. The cDNA sequence tACC2 of the *LE-ACC2* gene (*9*) was inserted in reverse orientation between the CaMV 35*S* promoter and the nopaline synthase (NOS) terminator into the vector pBI101. Restriction sites are as follows: P, Pst I; S, Sal I; B, Bam HI; E, Eco RI; and Sc, Sac I. Transcription start is at +1. (**B**) Southern blot analysis. Total DNA (5 μg) from untransformed and transformed plants (*23*) (R1 generation) was digested with Eco RI and Pst I and hybridized (*24*) with a 657-bp fragment from the fourth exon of the *LE-ACC2* gene. Lane 1, untransformed; lane 2, homozygous antisense; and lane 3, heterozygous antisense plants. Hybridizing fragments correspond to the endogenous (*LE-ACC2*) gene at 3.0 kb and the antisense (PO35) gene at 1.7 kb. The 2.5-kb hybridizing fragment in lanes 2 and 3 is due to partial digestion.

Plant Gene Expression Center, University of California at Berkeley–United States Department of Agriculture, Albany, CA 94710.

*Present address: Department of Horticulture, Washington State University, Pullman, WA 94164.
†Present address: Cetus Corp., Emeryville, CA 94608.
‡To whom correspondence should be addressed.